I give permission for public access to my thesis and for copying to be done at the discretion of the archives' librarian and/or the College library.

_____ _____

Signature Date

# Regulation of *Drosophila* Fat Body Remodeling by Brain-secreted *Drosophila* Insulin-Like Peptides During Metamorphosis

by

Jennie (Xiang) Li

A Paper Presented to the

Faculty of Mount Holyoke College in

Partial Fulfillment of the Requirements for

the Degree of Bachelors of Arts with

Honor

Program in Biochemistry

South Hadley, MA 01075

May 2022

This paper was prepared

under the direction of

Professor Craig Woodard

For eight credits

# ACKNOWLEDGEMENTS

I would like to thank my research advisor Prof. Craig Woodard for offering me this valuable research opportunity. Your tireless support, immense guidance, and thoughtful kindness enabled me to pursue an honors project within a year. More than an excellent researcher and professor, you are an admirable mentor, willing to give all your effort to support my personal growth in every aspect of my life.

I would also like to express my sincere gratitude to everyone who has enabled the success of this project. Thank you to Prof. Katie Berry and Prof. Kenneth Colodner for being on my committee and reviewing my thesis work. I genuinely appreciate Prof. Colodner's contribution with his immense knowledge of flies and neuroscience. The initial fly stocks from Prof. Colodner enabled me to start this project. Thank you to Clarie Pless for her patience in providing me with extensive training in microscopy that allowed me to capture beautiful dissection images and overcome numerous technical difficulties. Thank you to Prof. Laurie Tupper for her generous support in performing and presenting statistical analysis in my thesis. Thank you to Jerry Shan, who offered enormous help with code writing and program designing that enabled me to complete the major highlight of my thesis work.

I thank my fellow labmates Coco Zhai, Ceren Citak, and others for listening to my presentation, bringing up excellent suggestions, and giving me great encouragement. It was my pleasure to work with you all.

I want to express my gratitude to Kesshni Bhasiin, Yuxi Zhu, Siyu Sun, Rebecca Zhai, and numerous friends who have warmed me and cheered me through the ups and downs in my life. Thank you to Kessh for her extensive support in polishing my thesis, essays, and resume, which greatly facilitated my success in several critical stages of my college career. Thank you to James Burke and Amedeo DeCara, who devoted time and effort to studying essay formatting with me.

Lastly, I would like to thank my mom and dad. Your unconditional love and faith in me have given me great confidence and courage to face any challenge in my life.

# TABLE OF CONTENTS

# LIST OF FIGURES

# LIST OF TABLES

# ABSTRACT

Understanding the role of the brain in regulating peripheral metabolic activities may help unveil mechanisms underlying metabolic disorders. *Drosophila melanogaster* is a widely-used animal model for biological research, given its relatively inexpensive maintenance and short life cycle. Notably, during the critical developmental stage of metamorphosis in *Drosophila*, the peripheral adipose tissue, the larval fat body (FB), receives signals from three brain-secreted *Drosophila* Insulin-like Peptides (DILPs). This interaction is one form of brain-body communication, and I aimed to study the effects of DILPs on the progression of larval FB remodeling during metamorphosis.

To examine the same, I generated two groups of transgenic flies with enhanced and suppressed insulin secretion by insulin-producing neurons at 30˚C. Transgenic and wild-type pupae were collected at the beginning of metamorphosis, incubated at 30˚C to induce enhanced or suppressed DILP-secretion, and aged to different times after puparium formation (APF). Animals were then dissected to examine the degree of FB dissociation.

A new quantitative method was developed to quantify the percentage of FB dissociation. Through linear regression analysis, the rate of FB dissociation APF was compared across three genotypes. Our data suggested that transient change in DILP-secretion from the beginning of metamorphosis did not significantly affect FB remodeling.

# INTRODUCTION

Brain-body communication is crucial for many aspects of an organism's life. A recent study demonstrated that clusters of sharp-wave ripples in the mouse hippocampus during sleep could modulate blood-glucose homeostasis (Tingley et al., 2021). In addition to its function in memory consolidation, the occurrence of clustered sharp-wave ripples, which is one type of hippocampal output, can induce a decrease in peripheral glucose levels. Putative pathways of the metabolic function of sharp-wave ripples include direct innervation of the pancreas and liver, and/or regulation via hormones secreted by the hypothalamus that regulate insulin release and glucose homeostasis (Tingley et al., 2021). *Drosophila melanogaster* is an ideal model organism for examining the interaction between brain function and energy homeostasis. It has a short life cycle and is inexpensive to maintain (Moraes & Montagne, 2021). Importantly, many biological processes are conserved, and homologs of specific mammalian genes can be found in *Drosophila*, such as the *Drosophila* insulin receptor (Fernandez-Almonacid & Rosen, 1987). In *Drosophila*, one way of energy regulation is via brain-secreted insulin-like peptides that act on the peripheral adipose tissue called the fat body. The fat body is an organ that facilitates growth and development throughout the life of a fruit fly. During metamorphosis, it undergoes a critical transformation called remodeling, which resembles cancer metastasis. Thus, I was motivated to investigate the role of the brain in regulating the fat body in *Drosophila*, specifically the process of fat body remodeling.

## Insulin Signaling

Insulin and insulin-like growth factor (IGF) signaling is a complex system that modulates a wide range of processes, including metabolism/homeostasis, growth, development, stress responses, and aging/lifespan (Post et al., 2018). Insulin disturbance can lead to diseases such as diabetes and insulin resistance and may contribute to the progression of neurological disorders (Ghasemi et al., 2013). The Insulin and IGF signaling (IIS) pathways are highly conserved across a tremendous evolutionary distance from invertebrates to mammals (Graham & Pick, 2017; Sun et al., 2017). In *Drosophila melanogaster*, the IIS pathway is propagated by eight insulin-like peptides (DILP1-8), homologs of mammalian insulin and IGFs (Post et al., 2018). DILPs are recognized by the insulin/IGF receptor (InR), an ortholog of the human insulin receptor that activates conserved signal transduction and intracellular cascades (Fernandez-Almonacid & Rosen, 1987). Since *Drosophila melanogaster* is a well-studied research subject, it can serve as an ideal animal model for investigating the molecular mechanisms underlying the IIS pathway and providing insights into IIS dysfunction in human diseases.

DILP-induced insulin signaling is vital for *Drosophila* growth control (Figure 1). DILPs are produced and secreted by seven insulin-producing cells (IPCs) in the central nervous system, and ablation of the IPCs in larvae can lead to a systematic growth defect (Colombani et al., 2003). DILP-secretion is regulated by the peripheral adipose/liver tissue fat body in response to fat, sugar, and amino acid levels (Shim et al., 2013). The binding of DILP to the insulin/IGF receptor (InR) in peripheral tissues triggers a series of downstream cascades that regulate growth (Shim et al., 2013). First, phosphatidylinositol 3-kinase (PI3K) is activated by DILP binding, causing an increase in phosphatidylinositol 3,4,5 triphosphate (PIP3) levels

and mediating other members of this canonical pathway - lipid phosphatase PTEN, PDK1, and AKT. AKT inhibits two downstream targets, the Forkhead box transcription factor *Drosophila* Foxo (dFOXO) and the tumor suppressor proteins TSC1 and TSC2. dFOXO is related to growth and translation suppression. TSC1/ TSC2 complex represses Rheb GTPase, and Rheb activates *Drosophila* Tor (dTOR), an essential protein that promotes growth and inhibits autophagy. In summary, DILP-induced insulin signaling inhibits the dFOXO transcription factor and promotes dTOR, resulting in growth-promoting effects.

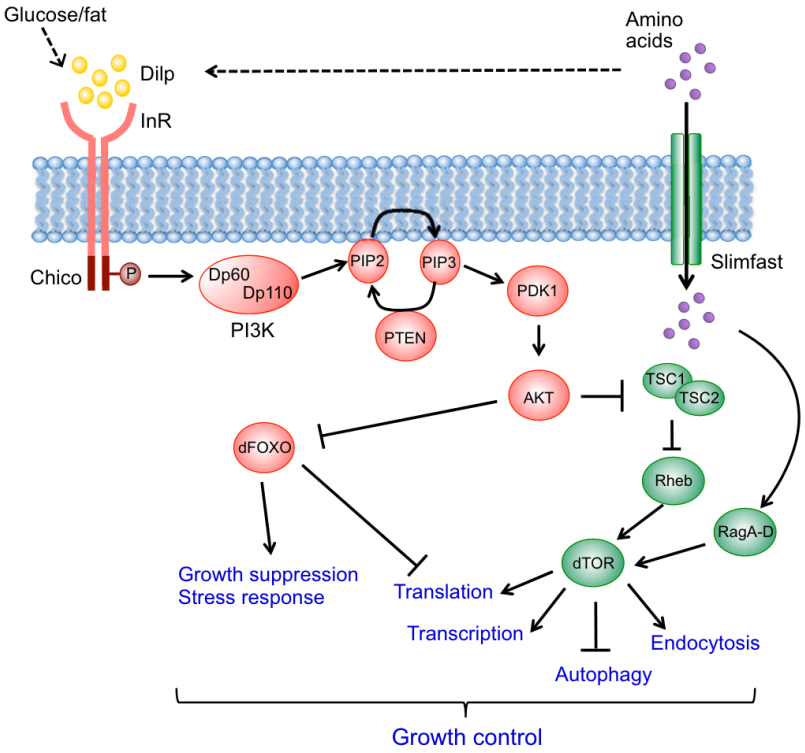


**Figure 1. DILP-induced insulin signaling in *Drosophila*.** High levels of sugar, fat, and amino acids lead to the secretion of *Drosophila* insulin-like peptides (DILPs) from brain insulin-producing cells. Circulating DILP can bind to the insulin receptor (InR) and transduction of this signal triggers signaling cascades including PI3K, PTEN, PDK1, and AKT. The downstream target dFOXO is inhibited by AKT. The repression of the TSC1/TSC2 complex activates Rheb and dTOR. In addition, amino acids are imported by the transporter Slimfast and can activate dTOR via RagA-D proteins. DILP-induced insulin signaling regulates multiple pathways regarding growth control. (Figure from Shim et al., 2013).

## *Drosophila* Insulin-like Peptides

Eight *Drosophila* Insulin-like Peptides (DILPs) have been identified. DILPs have various spatiotemporal expression patterns and functions and help coordinate nutritional status with systemic growth control (Zheng et al., 2016). DILP2, 3, and 5 are expressed in insulin-producing cells (IPCs) in the brain, which are functionally analogous to pancreatic beta cells in vertebrates (Shim et al., 2013). The IPC-synthesized DILPs signal to the peripheral fat body, the primary nutrient-responsive tissue which emulates the functions of the liver and adipose tissue of vertebrates (Colombani et al., 2003). DILPs secreted from neurons bind to InR in peripheral metabolic tissues and trigger downstream cascades crucial for energy maintenance and glucose homeostasis. With DILP signaling, digested food is converted to trehalose as an energy source and stored in the fat body of larvae. Under starvation or low levels of circulating sugar, adipokinetic hormone (AKH) triggers the release of trehalose into the hemolymph to provide energy (Zheng et al., 2016). Autophagy is one type of cellular response to the changes in nutrient levels, and it can be down-regulated through InR/class I phosphoinositide 3-kinase (PI3K) pathway (Scott et al., 2004). During metamorphosis, 20E signaling inhibits insulin signaling in the fat body, allowing the fat cells to undergo autophagy to release cellular components in support of the developing adults.

## Fat Body Cell Autophagy

Macroautophagy (autophagy) is a complicated self-degenerative process that can occur under many conditions. It is a catabolic process involved in organelle turnover, growth, aging, cell death, and nutrient mobilization under starvation (Rusten et al., 2004; Scott et al., 2004). Although autophagy plays an important role in programmed cell death, it is different from

apoptosis, the cellular self-destruction process (Fan & Zong, 2013; Tracy & Baehrecke, 2013). Cells undergoing autophagy contain double-layered intracellular membrane structures enclosing some cytoplasmic contents, forming autophagosomes (Figure 2). Autophagosomes then fuse with lysosomes to form autolysosomes, which allow enclosed intracellular materials to be digested by lysosomal proteases. This recycling process benefits cells by (1) removing damaged organelles and (2) offering the catabolites, such as amino acids and long-lived proteins, as internal energy sources and building blocks for cellular functions and biosynthesis (Fan & Zong, 2013). These functions have survival values and suggest that autophagy serves as a survival mechanism under stressful environmental conditions. Autophagy is upregulated in fat body cells (FBCs) during metamorphosis when the animal is in nutrient deprivation, and ßFTZ-F1 mediated 20E signaling plays a role in this upregulation (Chen, 2020; Notarangelo, 2014; Woldemeskel, 2014). It is known that starvation-induced autophagy can be repressed by components of the insulin/PI3K pathway (Rusten et al., 2004; Scott et al., 2004). Hence, the level of autophagy in fat body cells can serve as an indicator of insulin signaling.

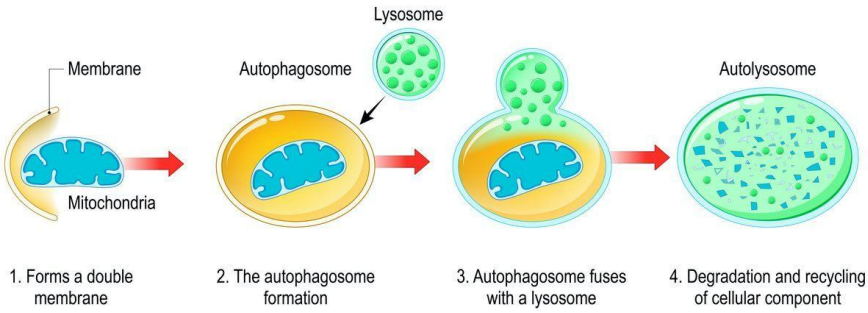


**Figure 2. The process of macroautophagy.** Autophagy is characterized by the formation of autophagosomes, which are cytosolic double-membrane vesicles containing cellular contents such as proteins, lipids, or damaged organelles. These structures then fuse with lysosomes to form autolysosomes with degraded cytoplasmic components. (Figure from Melchor 2021).

## *Drosophila* Metamorphosis

The life cycle of *Drosophila* consists of four major stages: embryo, larva (including first, second, and third instar larval stages), pupa, and adult (Figure 3). Metamorphosis is a critical phase in *Drosophila* development when a third instar larva undergoes critical transformations during the pupa stage to give rise to an adult. During metamorphosis, homeostasis is dynamically regulated to facilitate this drastic transformation, which requires the destruction of larval tissues and the proliferation of adult progenitor cells (Nelliot et al., 2006). Puparium formation (also called “pupariation”) occurs at the end of the third larval instar when the animal forms a pupal case (puparium) and begins metamorphosis. After puparium formation (APF), the pupa fasts for 4 to 5 days. During this period, the energy stored in the larval fat body is tightly controlled and released through various measures in contrast to active energy storage in an actively eating larva. 20E signaling and ßFZF1-mediated 20E signaling orchestrate the significant events of metamorphosis, including puparium formation, eversion

of adult heads, legs, and wings, destruction of larval body parts, and larval fat body remodeling.

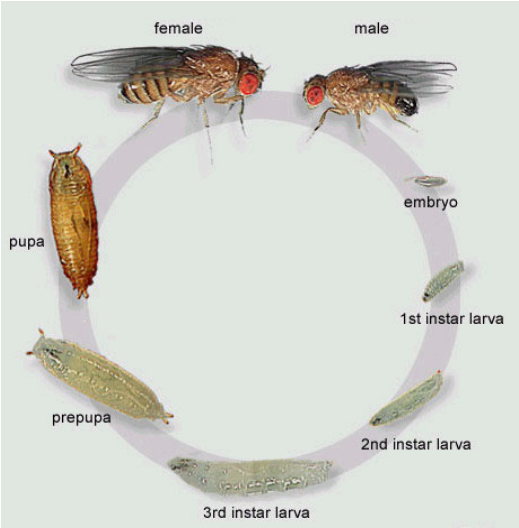


**Figure 3. The life cycle of *Drosophila melanogaster.*** The life cycle of a fruit fly lasts about 12 days at 25˚C. Beginning as an embryo, the animal hatches and undergoes three larval stages. Once it reaches critical weight by constant feeding and growing, the larva attaches to a substrate and becomes a white prepupa. This signifies the onset of metamorphosis, i.e., the transition from a larva to an adult. The pupa remains in the pupal case until eclosion into an adult fly. (Figure from Weigmann et al., 2003).

## Larval Fat Body Remodeling

The larval fat body (FB) is a functional homolog of the vertebrate adipocytes and liver (Colombani et al., 2003). In contrast to most larval tissues that undergo destruction during metamorphosis, the larval fat body, a major metabolic organ, is subject to a process called remodeling. Prior to metamorphosis, the larval fat body is composed of sheets of attached, polygonal cells suspended in the hemolymph between the body wall and the midgut. In the early stages of metamorphosis (6-12h after puparium formation), the fat body begins to dissociate, and fat cells become detached from each other, resulting in the redistribution of

individual fat cells throughout the body of the pupa (Figure 4). These dispersed fat cells eventually persist into adulthood and serve as nutrient reservoirs for newly eclosed adults (Bond et al., 2011; Nelliot et al., 2006). Throughout metamorphosis, a period of starvation, disaggregated fat cells are crucial for supplying energy for pupal survival and development. One major mechanism of energy release is via cell autophagy.

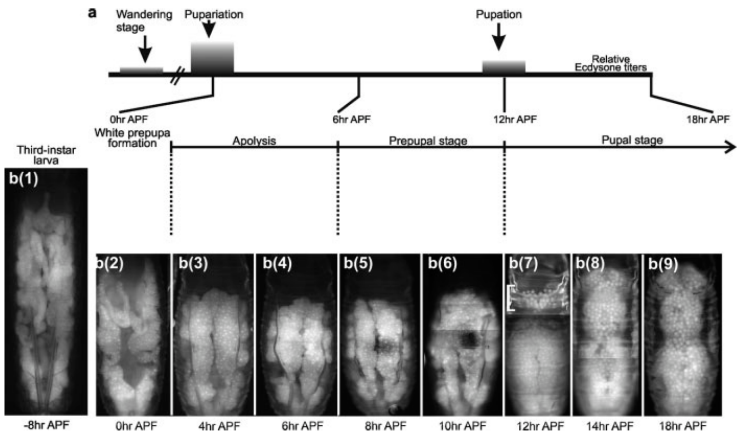


**Figure 4. Fat body remodeling in *Drosophila melanogaster*.** (a) Relative ecdysone titer in the whole animal during the late larval and early stages of metamorphosis. b(1–9) Changes in fat body morphology in whole animals viewed with fluorescence microscopy at different stages of metamorphosis. APF is the time after puparium formation at 25˚C. (Adapted from Nelliot et al., 2006).

## Regulation of Larval Fat Body Remodeling

FB remodeling is tightly regulated during *Drosophila* metamorphosis. Metamorphosis is developmentally regulated by the steroid hormone 20-hydroxyecdysone (20E), which binds to the ecdysone receptor to stimulate transitions between developmental stages (Bond et al., 2011). In the late third-larval instar, a surge in the 20E level induces the transcription of a set of “early genes”, which initiate metamorphosis and puparium formation. Following the brief

decline in 20E titer, the mid-prepupal genes are induced, and one of these genes encodes the competence factor ßFTZ-F1. ßFTZ-F1, in concert with the second pulse of 20E and the ecdysone receptor, induces the transcriptional cascades critical for prepupal to pupal transition. Matrix metalloproteinases (MMPs) are one type of the downstream targets of the ßFTZ-F1-mediated, 20E signaling cascade (Bond et al., 2011). MMPs are a specialized class of protease responsible for the degradation of the extracellular matrix (ECM) and allow for tissue remodeling. MMPs have been shown to be required for FB remodeling in *Drosophila* (Bond et al., 2011; Jia et al., 2014). Juvenile hormone (JH) and 20E coordinate control of the developmental timing of MMP-induced FB remodeling (Jia et al., 2017). JH signaling inhibits FB remodeling via JH primary-response gene Kr-h1 transduction that decreases MMP expressions during the larval-prepupal transition (0-6h APF).

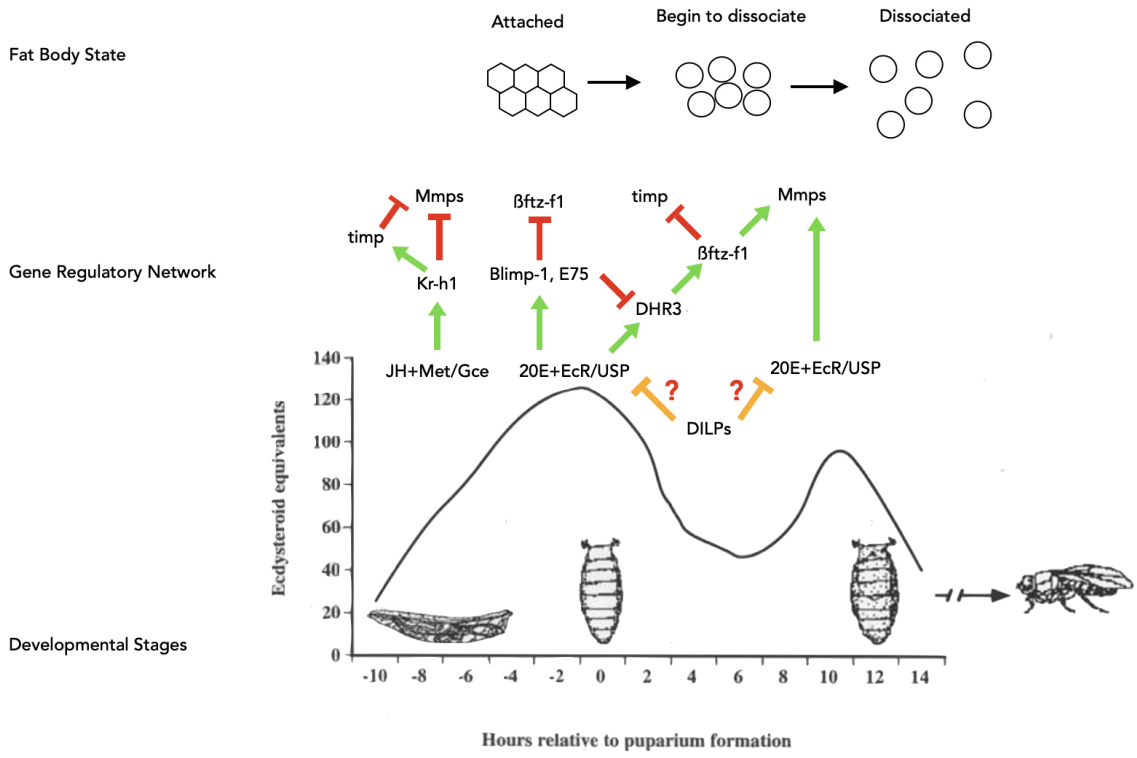


**Figure 5. Developmental timing and regulatory control of fat body remodeling.** During larval-prepupal transition JH signaling induces the anti-metamorphic factor Kr-h1, which directly inhibits Mmp expression and Mmp-induced fat body remodeling. As the JH titer declines, the first 20E pulse occurs at 0h APF and induces transcription of primary response genes, E75 and Blimp-1, which directly or indirectly inhibits the nuclear receptor ßftzf-1 expression. When the first 20E titer declines, ßftzf-1 expression is induced by 20 early-late response gene DHR3. ßftzf-1 and the second 20E pulse together activate Mmp expression and cause Mmp-induced fat body remodeling occurring from 6h APF to 12h APF. Given the evidence that insulin signaling inhibits 20E, we hypothesized that DILP signaling suppresses fat body remodeling through inhibition of 20E (Rusten et al., 2004; Scott et al., 2004). (Figure adapted from Jia et al. 2017 and Bond et al. 2011).

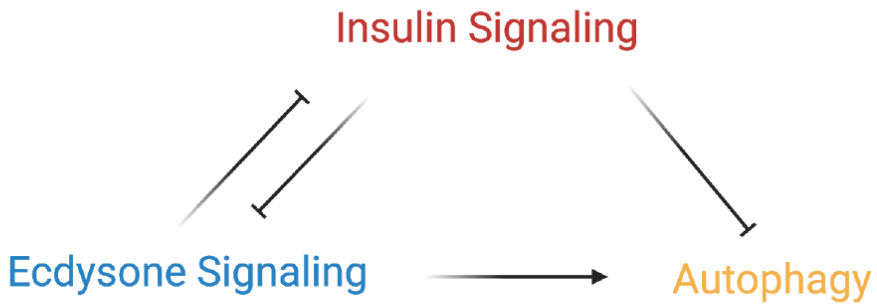


**Figure 6. Interaction between insulin signaling, ecdysone signaling, and fat body cells autophagy.** Insulin and ecdysone have antagonistic roles in regulating autophagy in fat body cells. Increased ecdysone level inhibits insulin signaling and promotes autophagy. Conversely, when insulin signaling increases, autophagy is suppressed through PI3K and TOR signaling, and ecdysteroid secretion is reduced. (Figure from Chen, 2020)

## Hypothesis and Aims

Given the importance of fat body remodeling in metamorphosis, I aim to investigate whether the *Drosophila* central nervous system is involved in regulating this process via DILP signaling. Previous findings have demonstrated an antagonistic relationship between insulin signaling and 20E/EcR signaling, which is regulated by the insulin/PI3K pathway (Orme & Leevers, 2005). As outlined above, ecdysone signaling induces fat body cell autophagy and promotes FB remodeling in the second pulse of 20E (Figure 5 & Figure 6). Therefore, I hypothesize that DILP signaling plays a role in inhibiting fat body remodeling by suppressing ecdysone signaling and fat body cell autophagy. For my thesis, I will examine this hypothesis by testing the prediction that enhancing neuron-secreted DILPs at the beginning of metamorphosis will inhibit FB remodeling. I will also test the prediction that suppressing neuron-secreted DILPs at the beginning of metamorphosis will promote FB remodeling.

By observing the percentage of FB dissociation at multiple time points from 0h to 15h APF, I expect to see delayed FB remodeling in the DILP-overexpressed group, and elevated FB remodeling in the DILP-suppressed group. If my hypothesis is supported, it will suggest that the central nervous system plays an essential role in FB remodeling through insulin signaling.

# MATERIALS AND METHODS

## *Drosophila* Stocks

All fly stocks were maintained on standard cornmeal media at 25˚C.

**Table 1. *Drosophila* stocks.**

| Name in this document | Genotype | Insertion location | Stock # | Provider |
|---|---|---|---|---|
| *Dilp5-GAL4* | *Ilp5-GAL4.L* | Chr 2 | 66007 | Bloomington *Drosophila* Stock center |
| *UAS-TrpA1$^{ts}$* | *UAS-TrpA1$^{ts}$* | Chr 2 | 26263 | Kenneth Colodner |
| *UAS-Shi$^{ts}$* | *UAS-Shi$^{ts}$* | Chr 3 | 44222 | Bloomington *Drosophila* Stock center |
| *w$^{1118}$* | *w$^{1118}$* | | N/A | Craig Woodard |

## *Drosophila* Culture Medium Preparation

(Be sure to wear goggles and gloves).

2L of tap water was boiled. Two bags of food mixture (Nutrifly Bloomington Formulation (BF), Genesee Scientific Catalog # 66-112) were added slowly to the boiling water. The food was boiled vigorously and stirred for 15 min. The pot was removed from the heater. After the temperature of the food cooled down to ≤ 80˚C, 20ml 10 mg/ml (in Ethanol) tegosept and 15ml propionic acid were added and mixed thoroughly. Food was then poured into clean vials and/or bottles.

## *GAL4/UAS* Binary System

The bipartite *GAL4/UAS* system was used to produce insulin-enhanced or suppressed pupae (Figure 7). The *GAL4/UAS* system is a common genetic tool that allows for the selective expression of target genes in specific cell types. It is composed of the GAL4 yeast transcription factor, and the Upstream Activation Sequence (*UAS*), a 17 base-pair GAL4-binding site (Duffy, 2002). When the GAL4 protein is produced under the control of a tissue-specific promoter, it binds to *UAS*, which subsequently induces expression of the target gene located downstream of *UAS*. For flexibility of manipulation and maintenance of stocks in the case of a lethal or toxic transgene, the transcription activator and the target gene are separated into two different transgenic fly lines. The GAL4 driver line carries the *GAL4* gene and a tissue-specific promoter. For example, in *Dilp5-Gal4*, the *GAL4* gene is located downstream of the Dilp5 promoter which can only be activated by Dilp5-producing cells, so *GAL4* is only expressed in the DILP-secreting neurons (Figure 7). The *UAS* reporter line carries *UAS* and the target gene. When both the *GAL4* and *UAS* constructs are present in the genome of the $F_1$ progeny of the *Dilp5-Gal4* x *UAS-target gene*, the target gene is expressed in the desired tissue (Duffy, 2002).

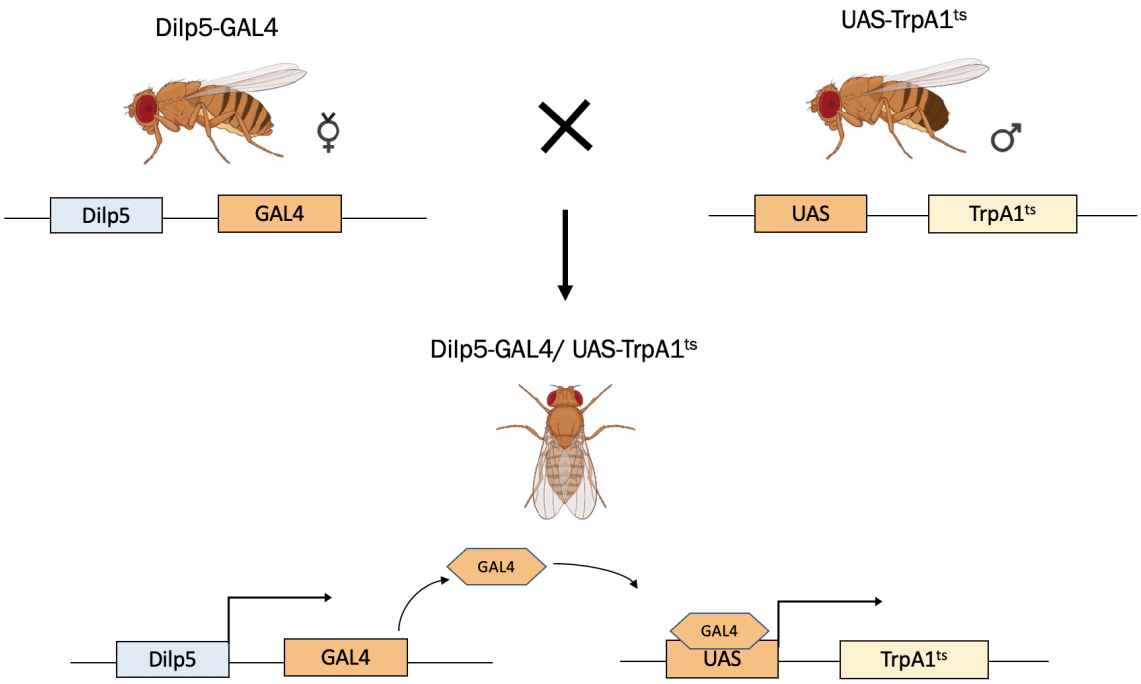


**Figure 7. The *GAL4-UAS* system with the transgenes of *Dilp5-GAL4* and *UAS-TrpA1$^{ts}$*.** Homozygous females carrying *Dilp5-GAL4* driver are mated with homozygous males carrying *UAS-TrpA1$^{ts}$* reporter. All F1 progenies contain both transgenes that result in specific expression of TrpA1$^{ts}$ in the DILP-secreting neurons.

## Transgenes

To manipulate the secretion of DILPs with temporal precision, transgenic *Drosophila* lines expressing different temperature-sensitive proteins in DILP-producing neurons were generated using the *GAL4/UAS* binary system.

TRPA1(transient receptor potential ankyrin 1) is a $Ca^{2+}$-permeable, non-selective cation channel which belongs to the Transient Receptor Potential (TRP) cation channel family (Kim et al., 2010). In *Drosophila*, TRPA1 is thermally activated by warm temperatures. By crossing *Ilp5-GAL4* with *UAS-TrpA1$^{TS}$*, the progeny *Ilp5-TrpA1$^{TS}$* expressed temperature-sensitive calcium channels TrpA1 in DILP-producing neurons. At temperatures higher than 26˚C, the TrpA1 channels opened, stimulating these neurons to release DILPs at higher levels than normal.

The Shibire$^{ts}$ protein is a temperature-sensitive mutant of the dynamin protein (Kohsaka & Nose, 2021). The *Shibire* mutant resulted in paralysis at high temperatures (Grigliatti et al. 1973). Crossing *Ilp5-GAL4* with *UAS-Shi$^{ts}$* yields progeny with genotype *Ilp5-Shi$^{ts}$*, expressing Shibire$^{ts}$ in DILP-producing neurons (Kohsaka & Nose, 2021). Since Shibire$^{ts}$ blocked endocytosis at temperatures higher than 30 °C, the vesicular neurotransmission in *Ilp5-Shi$^{ts}$* progeny was inhibited, suppressing DILP release than normal.

## Virgin Female Fly Collection

Flies from stock vials were transferred into bottles to maximize the production of progeny. Adults were removed once enough larvae were present. Cotton balls were placed into the

food at the bottom of the bottle using a clean wooden stick. All flies were removed 8-10 hours before collecting. The surface of the food was inspected to ensure the complete removal of flies. Flies were maintained at 18°C. Collected all eclosed female adults within 18 hours to ensure that all females would remain virgins.

## Fly Crossing

Adapted from Berg (2015).

Virgins of *Dilp5-GAL4* stock and males from the *UAS-TrpA1$^{TS}$* and *UAS-Shi$^{TS}$* were collected. Crosses were performed as illustrated in Figure 8. For each cross, ten virgins and ten males were placed into the same vial (1:1 ratio). All crosses were kept at 18˚C. After collecting the 0h prepupae, the prepupae were incubated at 30˚C. Adults were removed once enough larvae were present.

$$Ilp5-GAL4(2) \times UAS-TrpA1^{TS}(2)$$

$$\Downarrow$$

$$(A) \quad \frac{Ilp5-GAL4}{UAS-TrpA1^{TS}}$$

$$Ilp5-GAL4(2) \times UAS-Shi^{TS}(3)$$

$$\Downarrow$$

$$(B) \quad \frac{Ilp5-GAL4}{+} \; ; \; \frac{UAS-Shi^{TS}}{+}$$

$$Ilp5-GAL4(2) \times w^{1118}$$

$$\Downarrow$$

$$(C) \quad \frac{Ilp5-GAL4}{+}$$

**Figure 8. Cross scheme for generating transgenic flies.** (**A**) Crossing *Ilp5-GAL4* with *UAS-TrpA1*$^{TS}$ to generate a strain that expresses temperature-sensitive TrpA1 channels in neurons that secretes DILP 2, 3, and 5. At 30˚C, the opening of TrpA1 causes excessive excitation in these neurons and stimulates DILP secretion. (**B**) Crossing *Ilp5-GAL4* with *UAS-TrpA1*$^{TS}$ to generate a strain that expresses *Shibire* in DILP-producing neurons. At temperatures above 30˚C, the vesicular neurotransmission is inhibited, resulting in lower DILP secretion than normal. (**C**) Crossing *Ilp5-GAL4* with $w^{1118}$ to generate a strain that serves as the control. The control does not have abnormalities in DILP secretion. Numbers in parentheses indicate the insertion location.

## Larval Fat Body Dissection

Pupae collected as white 0h prepupa were placed on wet filter paper in a Petri dish at 30˚C, aged to 3h, 6h, 9h, 12h, 15h APF. A few drops of 1.0x Phosphate buffered saline (PBS) were added onto a glass slide under the Nikon Stereomicroscope. The animal was placed in the solution and dissection was performed. Images were captured by the camera on the microscope. To reduce the systematic error caused by variation in dissection skill and performance, dissection was performed with alternating genotypes across different days.

## Quantification of Larval Fat Body Remodeling

All the FB tissue of a single animal was gathered under the central field of vision for taking microscopy images. The images were processed using the ImageJ program. Given that the average FB cell size at 3h APF was approximately 2500 $\mu m^2$, a FB tissue larger than 10,000 $\mu m^2$ (4 or more cells in tissue) was considered non-dissociated. Area Total was the total area of FB tissue of each dissected animal. The area of dissociated FB tissue (Area dissociated) was measured at different developmental stages. Dissociation (%) = Area dissociated/Area total * 100. For analyzing the progression of fat body cell dissociation of each genotype from 0h to 15h APF, 27 animals were used for each genotype. A python script was used to automatically complete the calculation, organize data, fit linear regression models, and generate plots. The difference in the slopes of linear models of three groups was assessed with R by fitting a multiple regression model with the interaction of APF and genotype (R Core Team, 2022).

The following model was fitted to the data:

$$\widehat{Dissociation} = b_0 + b_1\, APF + b_2\, I_{TrpA1} + b_3\, I_{WT} + b_4 APF * I_{TrpA1} + b_5 APF * I_{WT}$$

This model contained a term for hours APF, the adjustment terms for each genotype (using Shi genotype as the baseline), and the interaction terms for APF and each genotype.

The full manuscript was available on Github (Li, 2022).

# RESULTS

Metamorphosis is a critical developmental stage of the life of *Drosophila melanogaster* and it is tightly controlled by multiple signaling pathways. To determine the role of DILP-induced insulin signaling in larval fat body remodeling during metamorphosis, the percentage dissociation of the fat bodies of control, DILP-enhanced, and DILP-suppressed animals were quantified at multiple time points after puparium formation (APF). The transgenic animals were generated using the GAL4-UAS binary system, by crossing *Dilp5-GAL4* virgins with $w^{1118}$, *UAS-TrpA1*$^{TS}$, or *UAS-Shi*$^{TS}$ males. The progenies were collected as white 0h prepupae and incubated at 30˚C to enhance or suppress DILP secretion until dissection transiently. Stereomicroscopy images of dissected fat bodies of each animal were processed by ImageJ,and percentages of dissociation were computed and analyzed using a tailored python script.

## Representative Images of Larval Fat Body

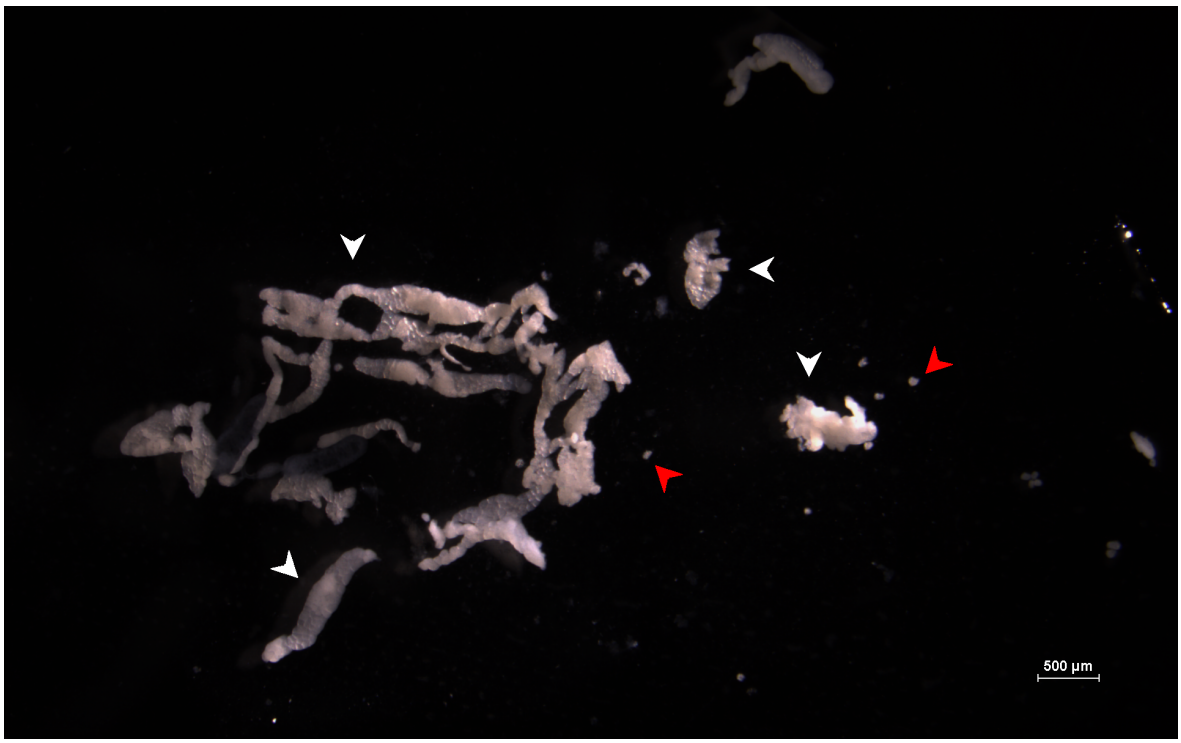


**Figure 9. Representative image of fat body of *Dilp5/+* pupa collected at 0h APF and dissected immediately under a stereomicroscope.** The animal was incubated at 18˚C prior to dissection. The fat body had not undergone remodeling and fat cells were tightly attached (white arrows) with only a few cells detached (red arrows). The percentage dissociation was found to be 2.10%. Image captured at 10x magnification.

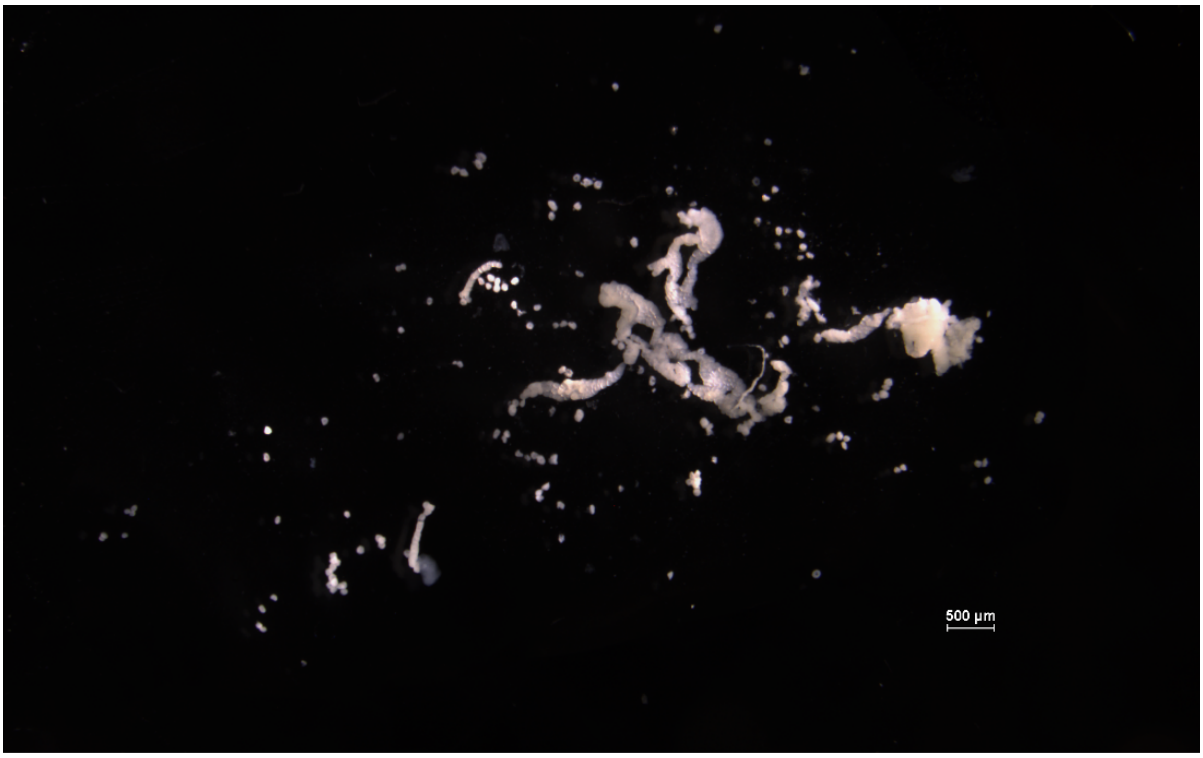


**Figure 10. Representative image of the fat body of *Dilp5/+* pupa collected at 0h APF and incubated at 30˚C until 3h APF.** The fat body had begun to dissociate and few fat cells had detached. The percentage dissociation was found to be 10.79%. Image captured at 7.5x magnification.

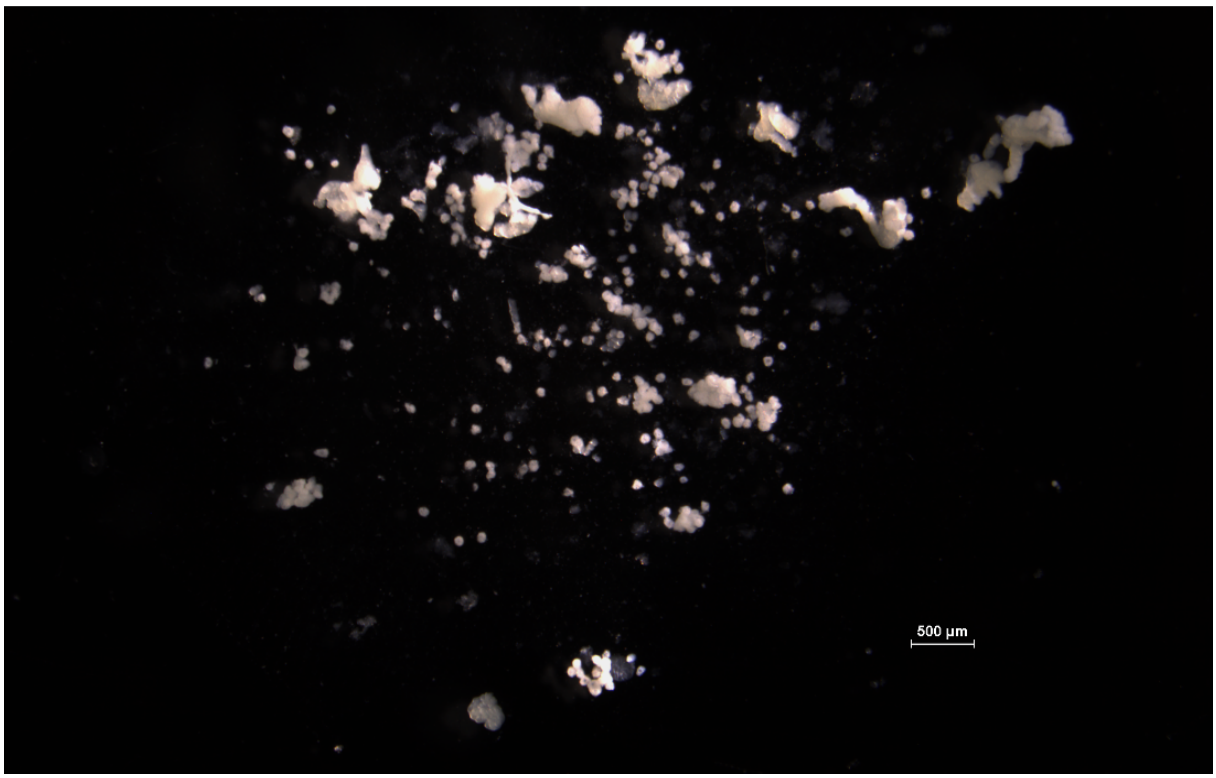


**Figure 11. Representative image of the fat body of *Dilp5/+* pupa collected at 0h APF and incubated at 30˚C until 7h APF.** The sheet of the fat body had dissociated into pieces. The percentage dissociation was found to be 13.62%. Image captured at 10x magnification.

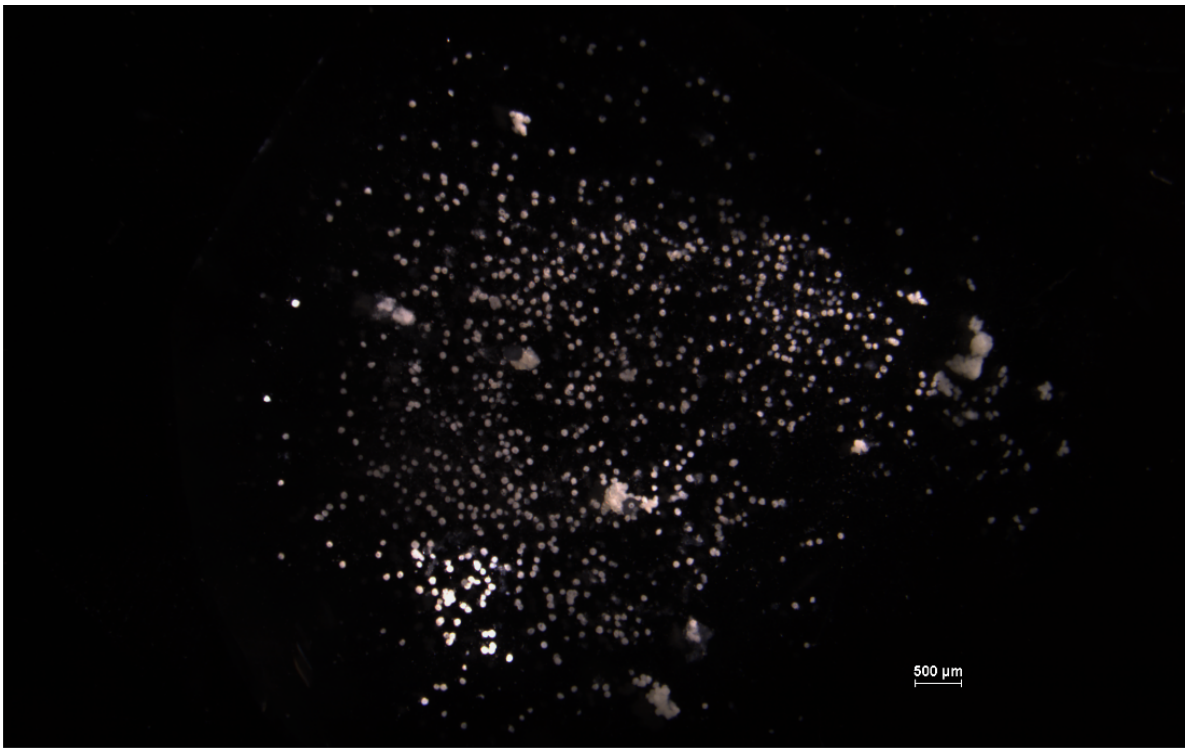


**Figure 12. Representative image of the fat body of *Dilp5/+* pupa collected at 0h APF and incubated at 30˚C until 11h APF.** The fat body was almost completely dissociated and few cells were attached. The percentage dissociation was found to be 55.44%. Image captured at 7.5x magnification.

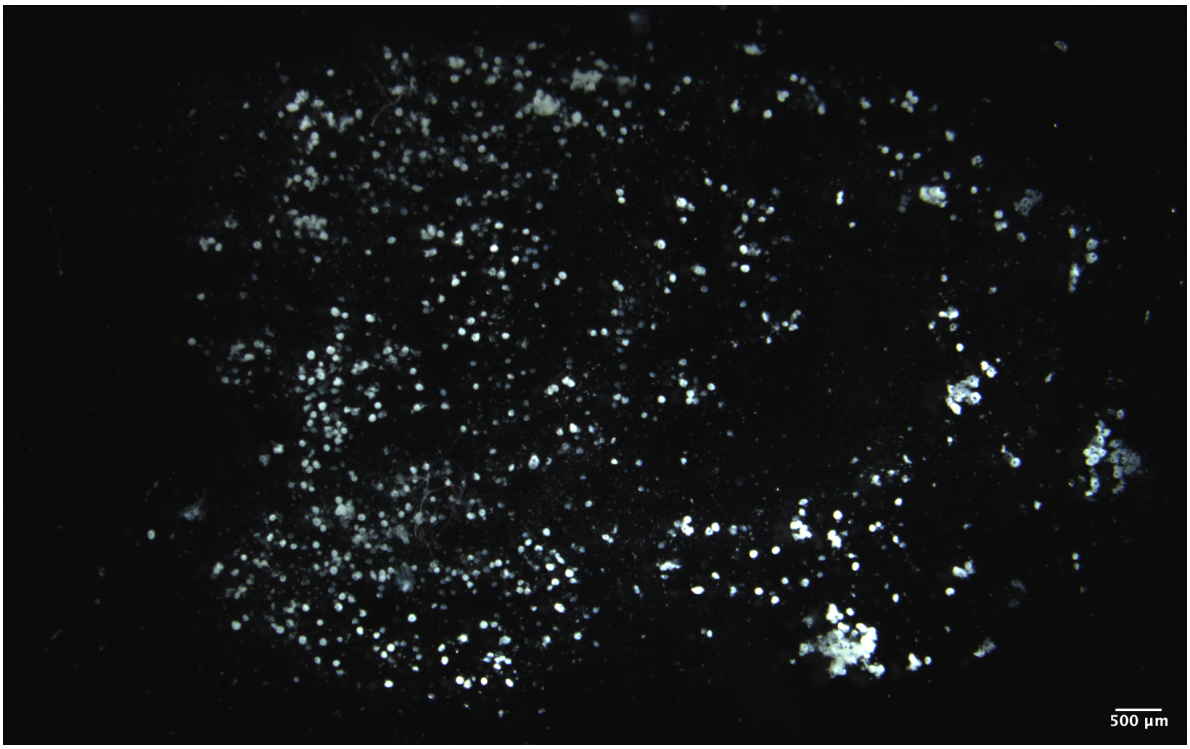


**Figure 13. Representative image of the fat body of *Dilp5/+* pupa collected at 0h APF and incubated at 30˚C until 14h APF.** The fat body was almost completely dissociated and few cells were attached. The percentage dissociation was found to be 44.12%. Image captured at 7.5x magnification.

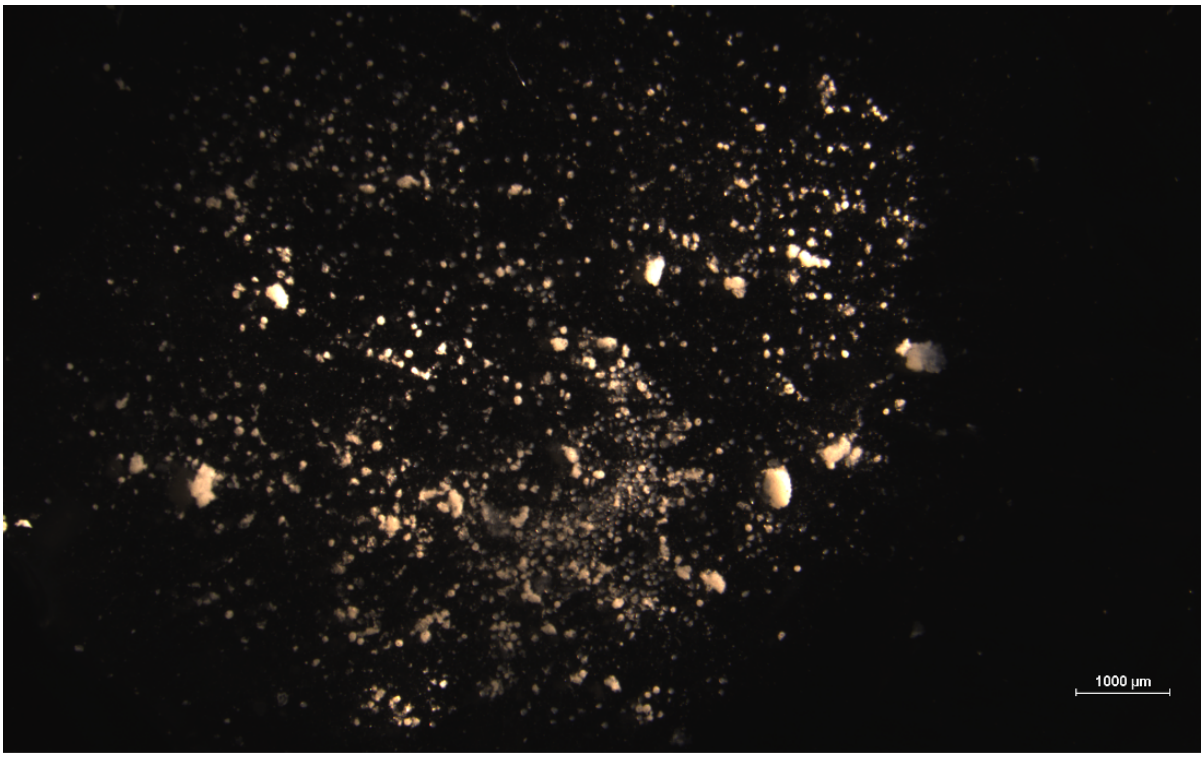


**Figure 14. Representative image of the fat body of *Dilp5/+* pupa collected at 0h APF and incubated at 30˚C until 15h APF.** The fat body was mostly dissociated. Some fat cells formed clumps. The percentage dissociation was found to be 54.72%. Image captured at 7.5x magnification.

## Linear Regression Analysis on Larval Fat Body Dissociation

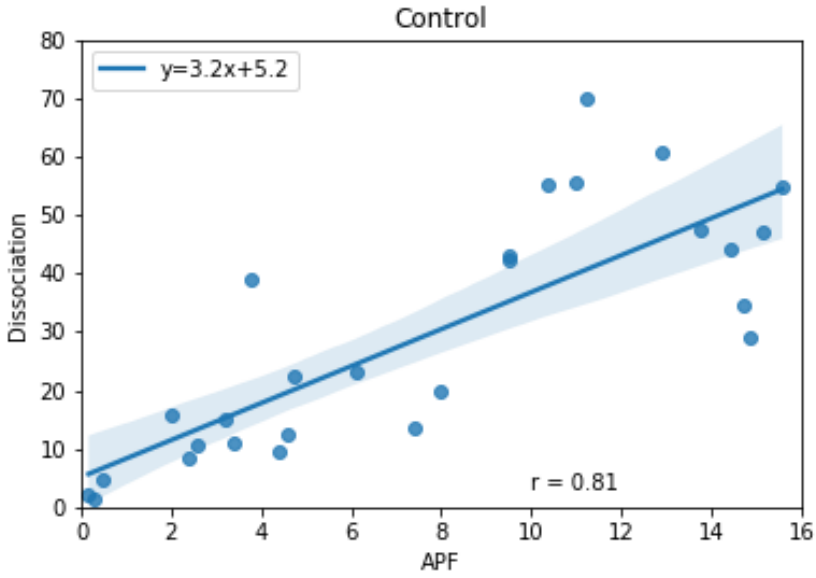


**Figure 15. Linear regression model for percentage fat body dissociation of *Dilp5/+* pupae against time after puparium formation (APF) under 30˚C.** Each dot represents an animal (n =27). The shaded region indicates standard error.

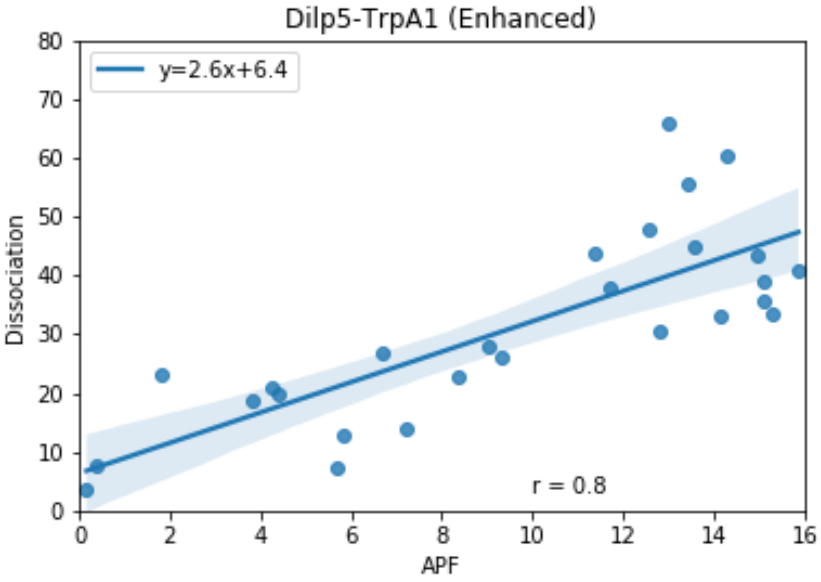


**Figure 16. Linear regression model for percentage fat body dissociation of *Dilp5-TrpA1$^{TS}$* pupae against time after puparium formation (APF) under 30˚C.** In these animals, the secretion of DILP 2, 3, and 5 was transiently stimulated at the beginning of metamorphosis. Each dot represents an animal (n =27). The shaded region indicates standard error.

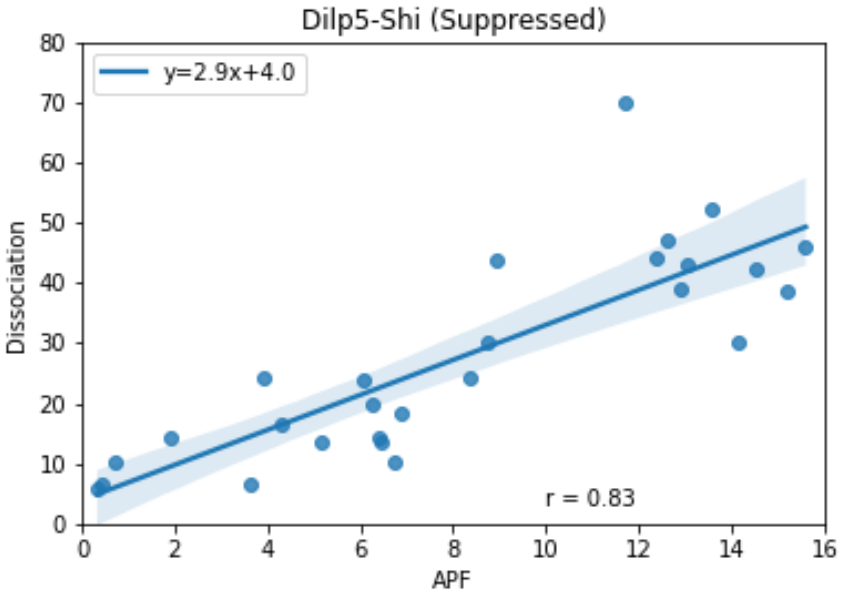


**Figure 17. Linear regression model for percentage fat body dissociation of *Dilp5-Shi$^{TS}$* pupae against time after puparium formation (APF) under 30˚C.** In these animals, the secretion of DILP 2, 3, and 5 was transiently suppressed at the beginning of metamorphosis. Each dot represents an animal (n =27). The shaded region indicates standard error.

## Quantitative Analysis of The Role of DILP 2, 3, And 5 In Regulating Larval Fat Body Remodeling During Metamorphosis

To evaluate the progression of *Drosophila* larval fat body remodeling in wild type control (Dilp5/+), DILP-overexpressed group (*Dilp5-TrpA1$^{TS}$*), and DILP-suppressed group (*Dilp5-Shi$^{TS}$*), the percentage of fat body dissociation was plotted over 0hrs to 15 hrs APF. Linear regression analysis was performed and the linear equation of each genotype was shown (Figure 15 - 17).

The statistical test was performed using R (Table 2). There was a significant correlation between hours APF and percentage dissociation ($p < 0.001$). This supports the validity of the

newly-developed quantification method. There were no statistically significant differences in the rate of fat body dissociation between wild-type control, *Dilp5-Shi*$^{TS}$, and *Dilp5-TrpA1*$^{TS}$ pupae incubated under 30˚C. While the estimated increase for the DILP-enhanced group is slightly lower than the DILP-suppressed group, and the estimated increase for the WT group is slightly higher than the DILP-suppressed group, the difference is not statistically significant ($p = 0.595$, $p = 0.665$). More data is required to confirm whether there truly exists a difference. The observed difference seems to agree with the hypothesis that secretion of DILP 2, 3, and 5 has a repressive effect on FB remodeling.

**Table 2. Summary of multiple regression statistics.** Output by R. In the last column, $p < 0.001$ indicates that the predictor is useful at predicting the percentage dissociation (indicated by *). Hours after puparium formation (APF) have a significant correlation with percentage dissociation. The adjusted R-square is 0.6385.

| | **Estimate** | **Std. Error** | **t value** | **p value** |
|---|---|---|---|---|
| (Intercept) | 4.007 | 4.087 | 0.981 | 0.330 |
| APF | 2.902 | 0.432 | 6.712 | 0.000 * |
| GenotypeDilp5-TrpA1 | 2.392 | 6.101 | 0.392 | 0.696 |
| GenotypeWT | 1.196 | 5.505 | 0.217 | 0.829 |
| APF:GenotypeDilp5-TrpA1 | -0.322 | 0.602 | -0.534 | 0.595 |
| APF:GenotypeWT | 0.256 | 0.590 | 0.435 | 0.665 |

# DISCUSSION

## A New Quantitative Approach to Assess Fat Body Remodeling

One major outcome of the present study is the development of a quantitative methodology to assess *Drosophila* larval FB remodeling. Stereomicroscopy images are processed to determine the area of each piece of tissue in the image. Then percentage dissociation is calculated using a python script and statistical analysis is performed using R. Statistical analysis shows that Hours After Puparium Formation (APF) reliably correlates with the percentage of larval FB dissociation (Table 2, $p < 0.001$), suggesting that the newly developed method indeed accurately quantifies FB dissociation. This new quantitative approach was used to experimentally test the hypothesis that DILPs inhibit larval fat body remodeling during metamorphosis.

## The Role of DILPs in Fat Body Remodeling

My hypothesis states that the central nervous system plays an important role in FB remodeling through DILP-induced insulin signaling. Specifically, I expect to see delayed FB remodeling when DILP 2, 3, and 5 are over-secreted and enhanced FB remodeling when DILPs are under-secreted, where DILP secretion of the animals is transiently changed at the beginning of metamorphosis (0h APF) up to 15h APF. Having determined that the new quantitative analysis is a reliable and useful approach, I applied the methodology to quantify FB dissociation in control, DILP-overexpressed, and DILP-suppressed animals. However, the statistical analysis did not support the hypothesis. Genotype is not a predictor of FB dissociation when hours APF is accounted for (Table 2, $p > 0.05$).

The result suggests that DILP-induced insulin signaling might not affect fat body remodeling. Another possible explanation is that the transient change in DILP secretion is negligible and hence failed to produce an effect on fat body remodeling. Moreover, the lack of statistical significance might be due to small sample sizes. With increasing sample sizes, the noticeable difference between the rate of dissociation of the three groups might be more concrete. Importantly, there is a lack of biomedical evidence of excessive or deficient DILP secretion in the experimental groups. To detect the actual secretion of DILPs, antibodies targeting DILPs can be applied to allow for immunofluorescence quantification and/or western blot analysis. A potential solution is proposed below in Future Directions. If the method used in this study failed to manipulate DILP secretion, then alternative methods are required.

## Limitations and Problems

A previous publication states that about 80% of the fat body was remodeled by 12h APF for pupae incubated at 25˚C (Jia et al., 2014). My study, which used rigorous quantify analysis, yields slightly lower percentages. There are several possible reasons for this. One, clumps are found in all three genotypes at 13 to 15h APF (Figure 18 - 20). At an advanced stage of 15h APF, we see clumps that were not completely dissociated. The clumps of cells seem to be held together by contents that look like extracellular matrices. Two, the different incubation temperatures are different (25˚C vs. 30˚C). Abnormally high temperatures might disrupt the development of pupae and cause abnormality in FB dissociation, in addition to simply increasing the rate of growth. Experiments are proposed to address this issue (see Future Directions). Three, the uniformity of dissection performance drastically affects the result by

causing unstable artificial destruction of the tissue across samples. Extensive training on and practice with fat body dissection is necessary.

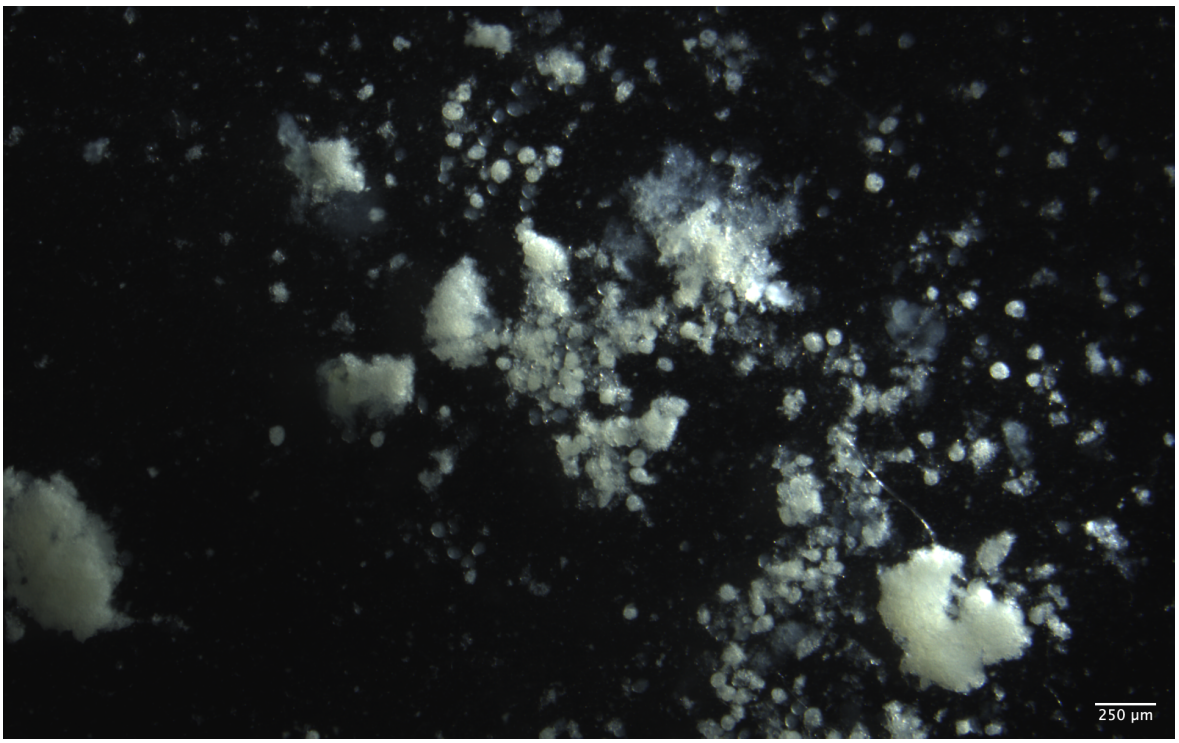


**Figure 18. Representative image of the fat body of a *Dilp5/+* pupa collected at 0h APF and incubated to 15h APF at 30˚C.** Image captured at 20x magnification. A clump of fat cells was shown.

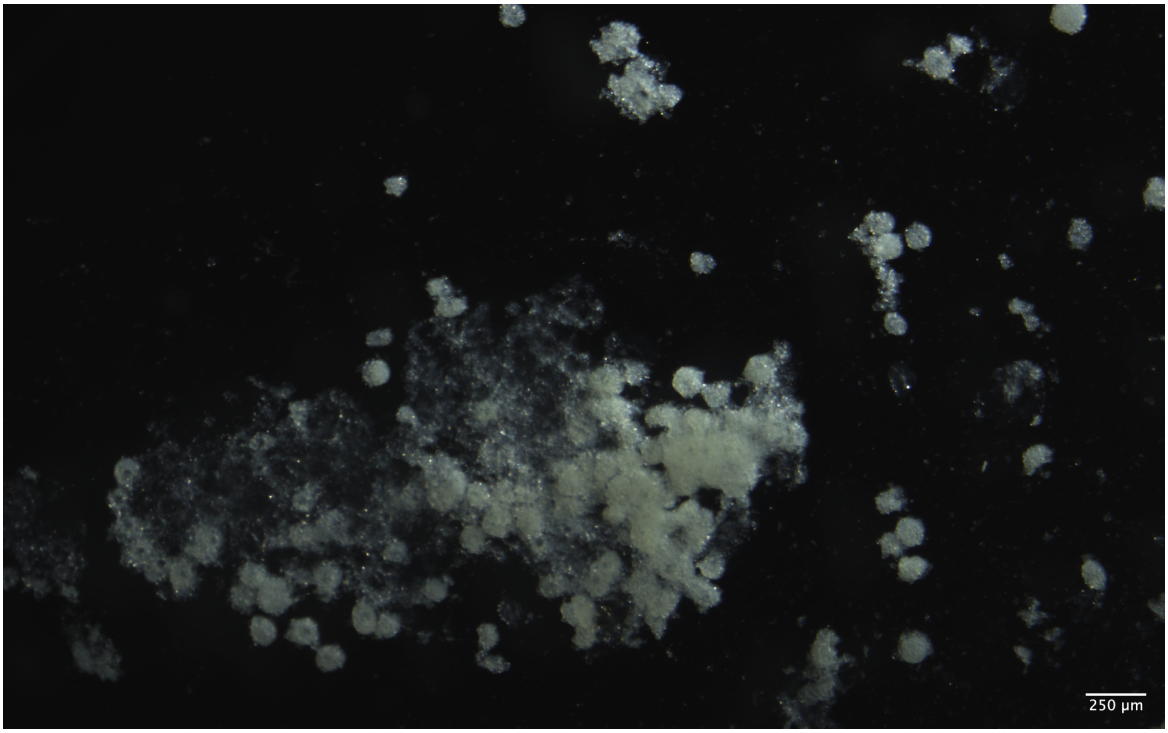


**Figure 19. Representative image of the fat body of a *Dilp5-TrpA1$^{TS}$* pupa collected at 0h APF and incubated to 15h APF at 30˚C.** Image captured at 20x magnification. The fat cells seemed to be entangled by the extracellular matrix.

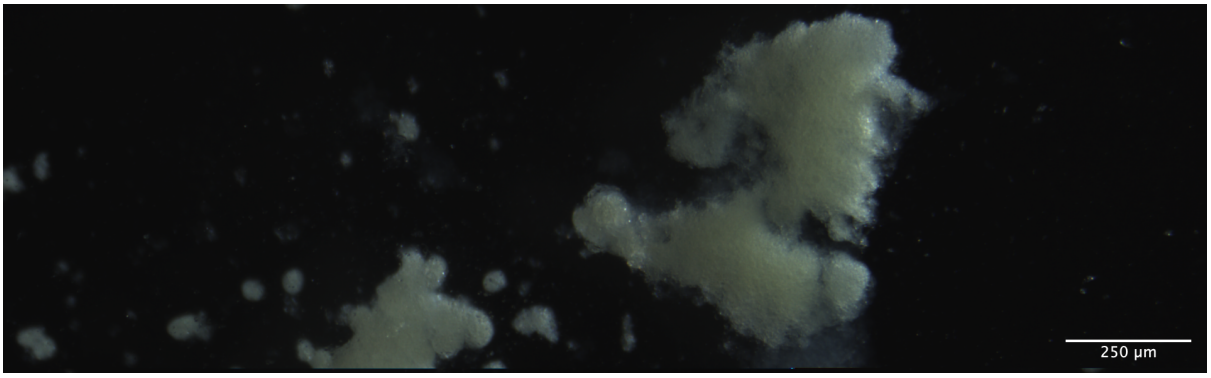


**Figure 20. Representative image of the fat body of a Dilp5-ShiTS pupa collected at 0h APF and incubated to 15h APF at 30˚C.** Image captured at 40x magnification.

## Future Directions

My newly developed method for quantifying *Drosophila* larval fat body can be applied to other settings and experiments. Researchers can take advantage of the open-access manual and codes to improve the accuracy and efficiency of their data analysis.

There are two approaches to address the issue of sample size. To better fit the linear model over a period of 0h to 15hrs, more data points are needed. Alternatively, given the limited sample size, one can increase the statistical strength of the data by collecting aggregated data points within particular time frames (3, 6, 9, 12, 15 hrs APF).

A promising approach to detecting DILP secretion is to use antibody staining. Dilp2- and Dilp5-specific antibodies are available, allowing for immunostaining and western blot analysis to detect and measure DILPs in tissue sections (Géminard et al., 2009). With antibodies designed against Dilp2 and Dilp5, one can use confocal microscopy to quantify fluorescence intensities for DILPs in the IPCs of larvae with suppositive enhanced or suppressed DILP secretion.

Additionally, more studies should be done to address the cause of the formation of clumps of fat cells in pupae incubated at 30˚C. Future studies can explore the effect of temperature on the development of *Drosophila* during metamorphosis. For instance, the rate of dissociation of $w^{1118}$ pupae incubated at 30˚C is compared to those incubated at 25˚C from 0hrs to 15hrs APF. Specifically, the presence of clumps should be carefully examined.

One way to avoid the potential interfering effect of high temperature is to use other transgenic lines that carry non-temperature driven constructs. Constructs such as *UAS-TrpML* and *UAS-KCNJ2*, which increases and inhibits neuronal activity at 25˚C accordingly, are available (Appendix B1). The progeny can be incubated at 18˚C and move to 25˚C to cause a transient change in DILP secretion.

In conclusion, my work provides a promising approach to understanding the role of the brain in regulating peripheral metabolic activity in *Drosophila*. The framework used in this study should be adopted by researchers and can serve as a guide for future research regarding larval fat body dissociation and insulin signaling.

# LITERATURE CITED

Berg, C. (2015, April 23). An introduction to fruit flies. *The Berg Lab*. https://depts.washington.edu/cberglab/wordpress/outreach/an-introduction-to-fruit-flies/

Bond, N. D., Nelliot, A., Bernardo, M. K., Ayerh, M. A., Gorski, K. A., Hoshizaki, D. K., & Woodard, C. T. (2011). SSFTZ-F1 and Matrix metalloproteinase 2 are required for fat-body remodeling in Drosophila. *Developmental Biology*, *360*(2), 286–296. https://doi.org/10.1016/j.ydbio.2011.09.015

Chen, R. (2020). *The Effect of Ecdysone Signaling on Autophagy in the Fat body of Drosophila melanogaster During Metamorphosis*.

Colombani, J., Raisin, S., Pantalacci, S., Radimerski, T., Montagne, J., & Léopold, P. (2003). A Nutrient Sensor Mechanism Controls Drosophila Growth. *Cell*, *114*(6), 739–749. https://doi.org/10.1016/S0092-8674(03)00713-X

Duffy, J. B. (2002). GAL4 system in Drosophila: A fly geneticist's swiss army knife. *Genesis*, *34*(1–2), 1–15. https://doi.org/10.1002/gene.10150

Fernandez-Almonacid, R., & Rosen, O. M. (1987). Structure and ligand specificity of the Drosophila melanogaster insulin receptor. *Molecular and Cellular Biology*, *7*(8), 2718–2727.

Géminard, C., Rulifson, E. J., & Léopold, P. (2009). Remote Control of Insulin Secretion by Fat Cells in Drosophila. *Cell Metabolism*, *10*(3), 199–207. https://doi.org/10.1016/j.cmet.2009.08.002

Ghasemi, R., Dargahi, L., Haeri, A., Moosavi, M., Mohamed, Z., & Ahmadiani, A. (2013). Brain Insulin Dysregulation: Implication for Neurological and Neuropsychiatric

Disorders. *Molecular Neurobiology*, *47*(3), 1045–1065. https://doi.org/10.1007/s12035-013-8404-z

Graham, P., & Pick, L. (2017). Drosophila as a Model for Diabetes and Diseases of Insulin Resistance. *Current Topics in Developmental Biology*, *121*, 397–419. https://doi.org/10.1016/bs.ctdb.2016.07.011

Jia, Q., Liu, S., Wen, D., Cheng, Y., Bendena, W. G., Wang, J., & Li, S. (2017). Juvenile hormone and 20-hydroxyecdysone coordinately control the developmental timing of matrix metalloproteinase–induced fat body cell dissociation. *Journal of Biological Chemistry*, *292*(52), 21504–21516. https://doi.org/10.1074/jbc.M117.818880

Jia, Q., Liu, Y., Liu, H., & Li, S. (2014). Mmp1 and Mmp2 cooperatively induce Drosophila fat body cell dissociation with distinct roles. *Scientific Reports*, *4*(1), 7535. https://doi.org/10.1038/srep07535

Kim, S. H., Lee, Y., Akitake, B., Woodward, O. M., Guggino, W. B., & Montell, C. (2010). Drosophila TRPA1 channel mediates chemical avoidance in gustatory receptor neurons. *Proceedings of the National Academy of Sciences*, *107*(18), 8440–8445. https://doi.org/10.1073/pnas.1001425107

Kohsaka, H., & Nose, A. (2021). Optogenetics in Drosophila. In H. Yawo, H. Kandori, A. Koizumi, & R. Kageyama (Eds.), *Optogenetics: Light-Sensing Proteins and Their Applications in Neuroscience and Beyond* (pp. 309–320). Springer Singapore. https://doi.org/10.1007/978-981-15-8763-4_19

Li, X. (2022). *Woodard Lab Fat Body Dissociation Quantification* [Python]. https://github.com/Jennie421/woodard-lab-fat-body-dissociation-quantification.git

Moraes, K. C. M., & Montagne, J. (2021). Drosophila melanogaster: A Powerful Tiny Animal Model for the Study of Metabolic Hepatic Diseases. *Frontiers in Physiology*,

*12*. https://www.frontiersin.org/article/10.3389/fphys.2021.728407

Nelliot, A., Bond, N., & Hoshizaki, D. K. (2006). Fat-body remodeling in Drosophila melanogaster. *Genesis*, *44*(8), 396–400. https://doi.org/10.1002/dvg.20229

Orme, M. H., & Leevers, S. J. (2005). Flies on steroids: The interplay between ecdysone and insulin signaling. *Cell Metabolism*, *2*(5), 277–278. https://doi.org/10.1016/j.cmet.2005.10.005

Post, S., Karashchuk, G., Wade, J. D., Sajid, W., De Meyts, P., & Tatar, M. (2018). Drosophila Insulin-Like Peptides DILP2 and DILP5 Differentially Stimulate Cell Signaling and Glycogen Phosphorylase to Regulate Longevity. *Frontiers in Endocrinology*, *9*, 245. https://doi.org/10.3389/fendo.2018.00245

R Core Team. (2022). *R: A language and environment for statistical computing.* R Foundation for Statistical Computing. https://www.R-project.org/

Rusten, T. E., Lindmo, K., Juhász, G., Sass, M., Seglen, P. O., Brech, A., & Stenmark, H. (2004). Programmed Autophagy in the Drosophila Fat Body Is Induced by Ecdysone through Regulation of the PI3K Pathway. *Developmental Cell*, *7*(2), 179–192. https://doi.org/10.1016/j.devcel.2004.07.005

Scott, R. C., Schuldiner, O., & Neufeld, T. P. (2004). Role and Regulation of Starvation-Induced Autophagy in the Drosophila Fat Body. *Developmental Cell*, *7*(2), 167–178. https://doi.org/10.1016/j.devcel.2004.07.009

Shim, J., Gururaja-Rao, S., & Banerjee, U. (2013). Nutritional regulation of stem and progenitor cells in Drosophila. *Development (Cambridge, England)*, *140*(23), 4647–4656. https://doi.org/10.1242/dev.079087

Sun, X., Chen, W.-D., & Wang, Y.-D. (2017). DAF-16/FOXO Transcription Factor in Aging and Longevity. *Frontiers in Pharmacology*, *8*, 548.

https://doi.org/10.3389/fphar.2017.00548

Tingley, D., McClain, K., Kaya, E., Carpenter, J., & Buzsáki, G. (2021). A metabolic function of the hippocampal sharp wave-ripple. *Nature*, *597*(7874), 82–86. https://doi.org/10.1038/s41586-021-03811-w

Zheng, H., Yang, X., & Xi, Y. (2016). Fat body remodeling and homeostasis control in Drosophila. *Life Sciences*, *167*, 22–31. https://doi.org/10.1016/j.lfs.2016.10.019

# Appendix A

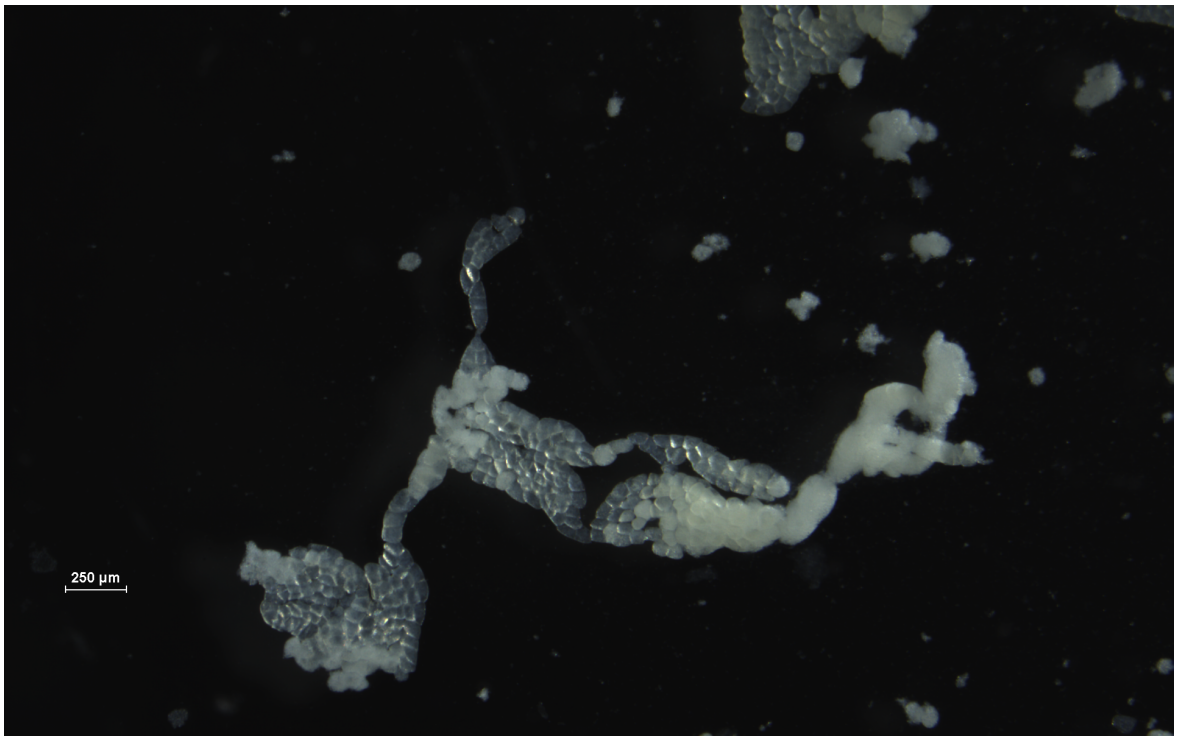


**Figure A1. Closeup image of the fat body of a *Dilp5/+* pupa collected at 0h APF and incubated to 3.4h APF at 30˚C.** Image captured at 20x magnification.

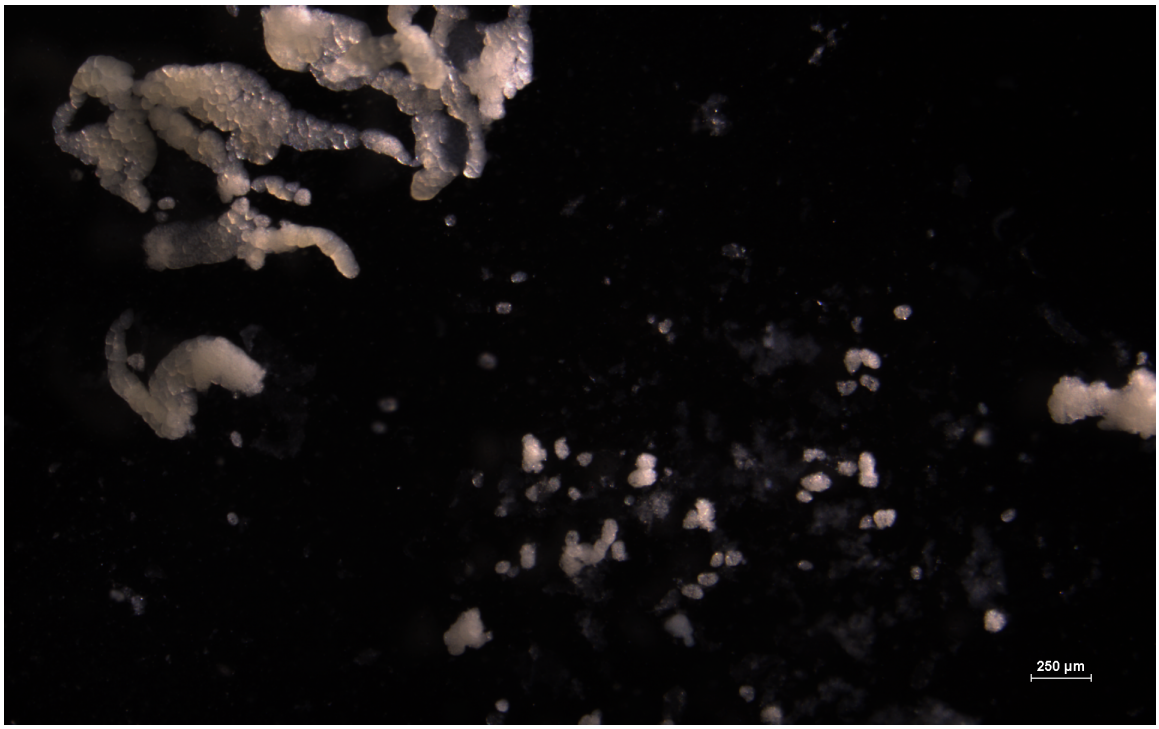


**Figure A2. Closeup image of the fat body of a *Dilp5/+* pupa collected at 0h APF and incubated to 4.4h APF at 30˚C.** Image captured at 20x magnification.

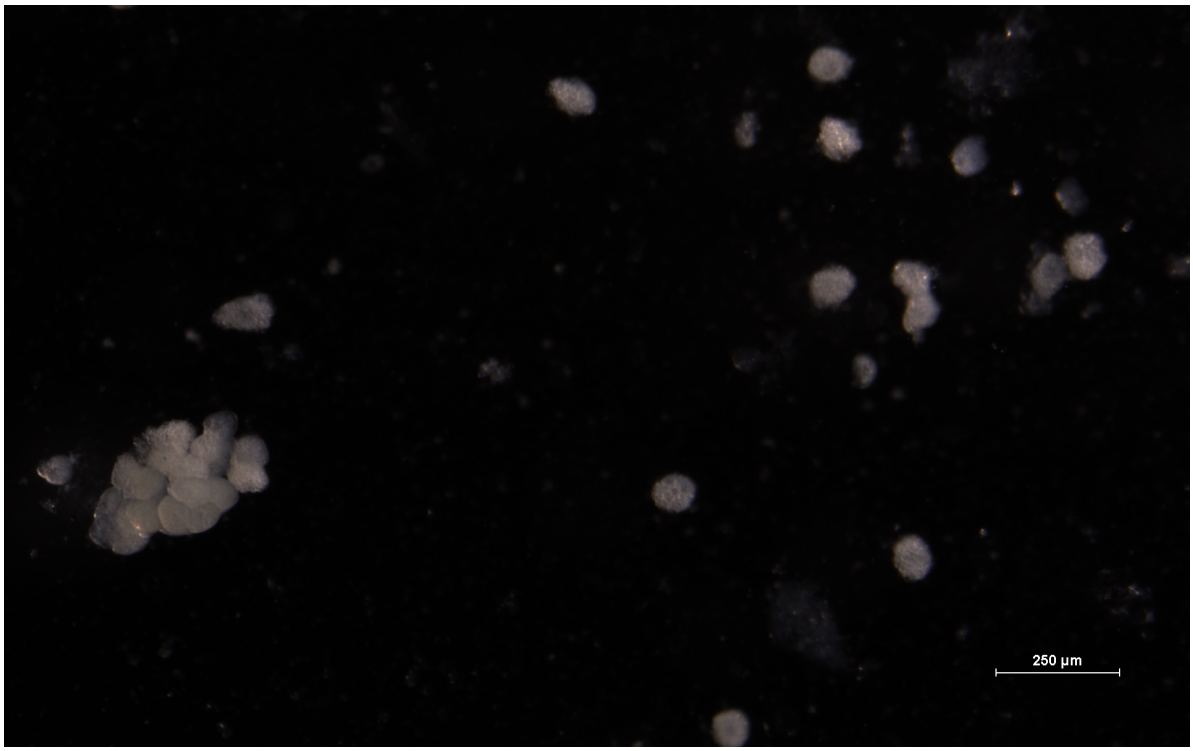


**Figure A3. Closeup image of the fat body of a *Dilp5/+* pupa collected at 0h APF and incubated to 7.4h APF at 30˚C.** Image captured at 40x magnification.

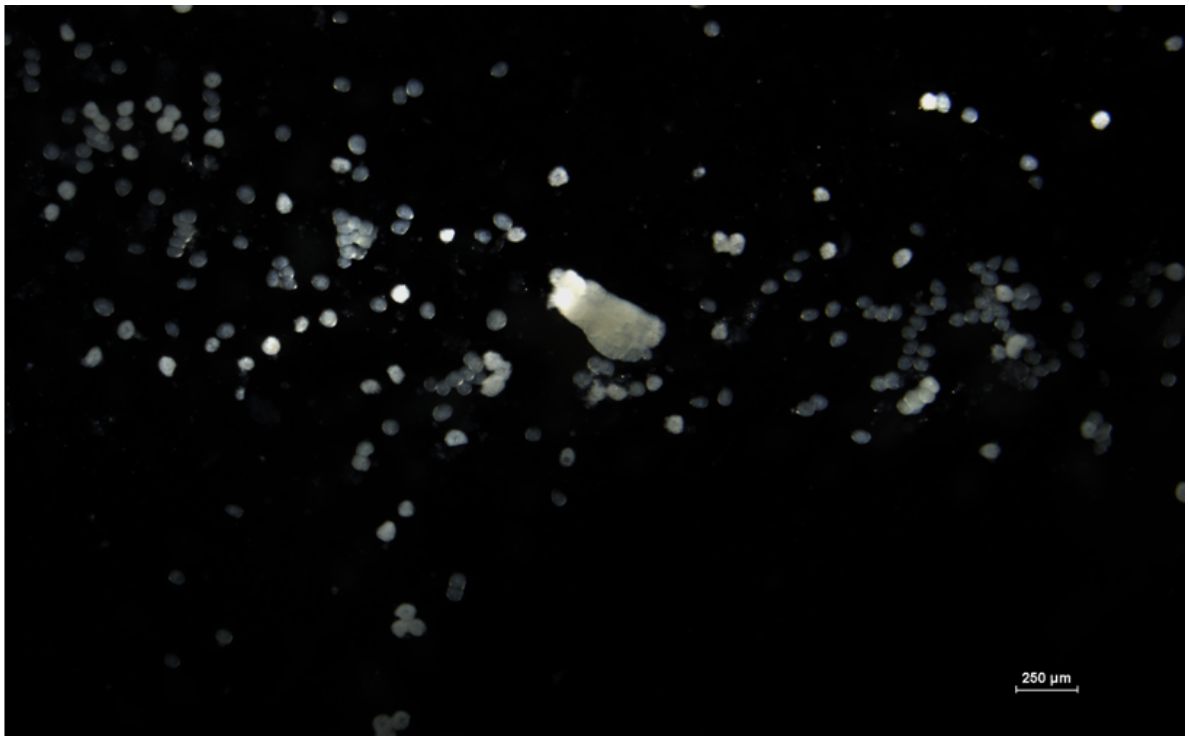


**Figure A4. Closeup image of the fat body of a *Dilp5/+* pupa collected at 0h APF and incubated to 9.5h APF at 30˚C.** Image captured at 20x magnification.

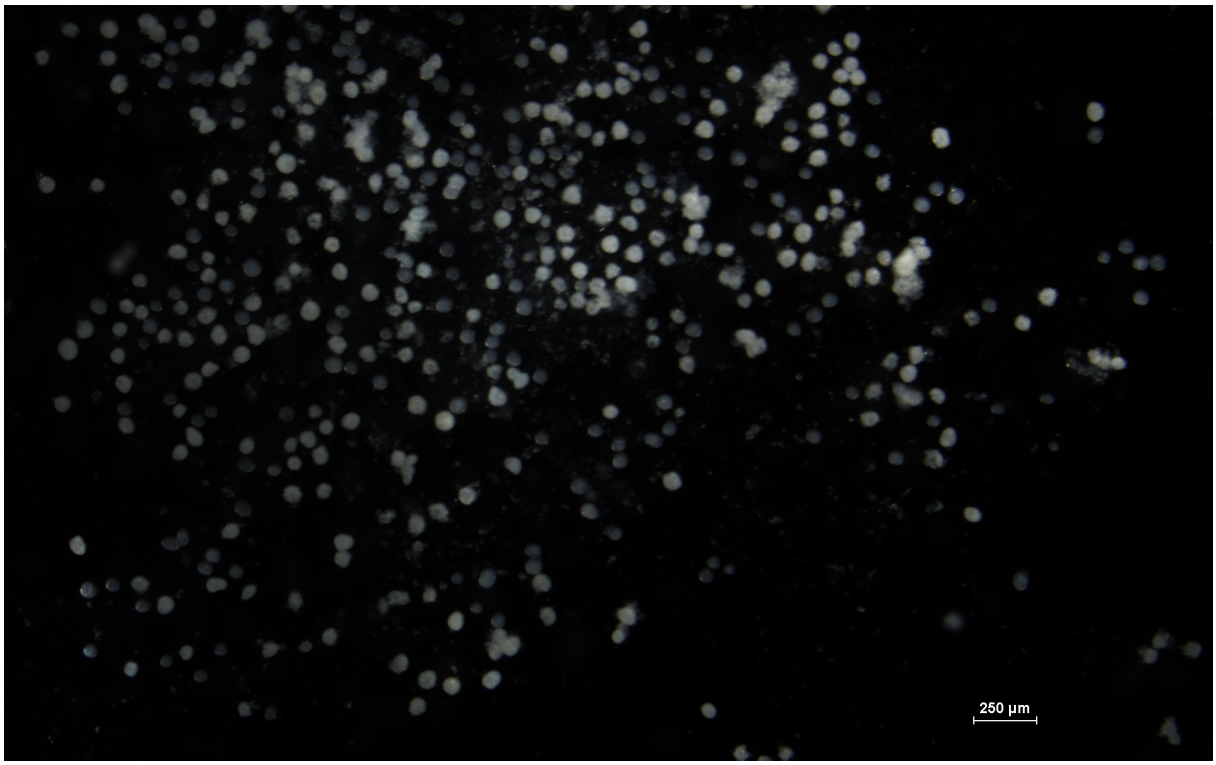


**Figure A5. Closeup image of the fat body of a *Dilp5/+* pupa collected at 0h APF and incubated to 10.4h APF at 30˚C.** Image captured at 20x magnification.

# Appendix B

**Table B1. Record of fly stocks.**

| Abbreviation | Genotype | Insertion location | Stock # | Provider |
|---|---|---|---|---|
| *Dilp2-GAL4* | *Ilp2-GAL4.R / CyO* | Chr 2R | 37516 | Bloomington Drosophila Stock center |
| *Dilp3-GAL4* | *Ilp3-GAL4.C / CyO* | Chr 2 | 52660 | Bloomington Drosophila Stock center |
| *Dilp5-GAL4* | *Ilp5-GAL4.L* | Chr 2 | 66007 | Bloomington Drosophila Stock center |
| *UAS-TrpA1$^{ts}$* | *UAS-TrpA1$^{ts}$* | Chr 2 | 26263 | Kenneth Colodner |
| *UAS-TrpML* | *UAS-TrpML.myc / TM6B, TB* | Chr 3 | 57372 | Kenneth Colodner |
| *UAS-Shi$^{ts}$* | *UAS-Shi$^{ts}$* | Chr 3 | 44222 | Bloomington Drosophila Stock center |
| *USA-Kir* | *USA-KCNJ2(Kir)* | Chr 2 | 6596 | Kenneth Colodner |
| *w$^{1118}$* | *w$^{1118}$* | | N/A | Craig Woodard |

**Table B2. Stereo Microscope magnification and scale.**

| Magnification | Conversion | Scale (pixels/unit) |
|---|---|---|
| 0.75x | 150 pixels = 1000 units | 0.15 |
| 1x | 100 pixels = 500 units | 0.2 |
| 2x | 100 pixels = 250 units | 0.4 |
| 4x | 200 pixels = 250 units | 0.8 |